IOP Conference Series: Materials Science and Engineering

PAPER • **OPEN ACCESS**

Preparation of In_2O_3@TiO_2 core-shell spherical nanocomposites with the enhanced photocatalytic activity under solar light irradiation

To cite this article: H M Zhao *et al* 2019 *IOP Conf. Ser.: Mater. Sci. Eng.* **504** 012037

View the article online for updates and enhancements.

This content was downloaded from IP address 117.93.176.10 on 14/10/2019 at 00:34

IOP Conf. Series: Materials Science and Engineering **504** (2019) 012037 doi:10.1088/1757-899X/504/1/012037

Preparation of In_2O_3@TiO_2 core-shell spherical nanocomposites with the enhanced photocatalytic activity under solar light irradiation

H M Zhao[1], H T Fu*[1,2], C X Ge[1] and Q Xu[1]

[1] School of Metallurgy, Northeastern University, Shenyang 110819, People's Republic of China
[2] Key Laboratory for Ecological Metallurgy of Multimetallic, Ministry of Education, Northeastern University, Shenyang, 110819, People's Republic of China

Corresponding author and e-mail: H T Fu, fuht@smm.neu.edu.cn

Abstract. In this study, we demonstrate In_2O_3@TiO_2 core-shell spherical nanocomposites prepared by hydrothermal method and sol-gel coating method. The In_2O_3 particles show quite a uniform particle size (~200 nm in diameter) and smooth surface. Porous TiO_2 polycrystalline is coated on the surface of In_2O_3 nanospheres as a shell. The thickness of the shell can be controlled by adjusting the molar ratios of In to Ti. UV-Vis spectra indicate that the adsorption peaks of pure In_2O_3 and TiO_2 nanospheres are located at 323 and 319 nm, respectively. The surface coating of TiO_2 can make the adsorption of nanocomposites shift to the long wavelength to ~340 nm. The photocatalytic activities of the pure In_2O_3, TiO_2, and the nanocomposites obtained with different molar ratios of In to Ti were evaluated by measurement of the degradation concentration of 30 ppm methylene blue (MB). The results show that the nanocomposites show higher photocatalytic performance than the pure oxides. The ratio at 1:10 exhibits the highest reaction rate constant (0.0152 min^{-1}), similar to other nanocomposites but higher than pure In_2O_3 nanospheres (0.0069 min^{-1}) and TiO_2 (0.0058 min^{-1}). This can be attributed to the large surface and tuned band energy structure for enhanced visible light absorption and the effective charge separation at the heterojunction of In_2O_3 and TiO_2. These findings may benefits to the new developed core-shell material as photocatalysts with enhanced efficiency for environmental applications.

1. Introduction

Photocatalysis is considered as an effective and low-cost way to solve the environmental issues, which become increasingly serious with the development of the industry.[1, 2] TiO_2, a traditional photocatalyst with high degradation efficiency, has attracted numerous attention since the evolution of oxygen and hydrogen from the TiO_2 electrodes has been reported by Fujishima and Honda in 1972.[3] Recently, it has been widely studied for the potential applications in air purification and photocatalytic degradation of organic pollutants due to its excellent chemical stability, low cost, and very low toxicity.[4-7] However, limited by the wide bandgap (~3.2 eV), TiO_2 is only excited by ultraviolet light which is <10% of the total solar spectrum irradiating to the surface of the earth.[8] Therefore, making TiO_2 responsive to visible light and enhancing the photocatalytic activity become major subjects for developing the TiO_2-based photocatalysts.[9-12] Many efforts have been made to extend

Content from this work may be used under the terms of the Creative Commons Attribution 3.0 licence. Any further distribution of this work must maintain attribution to the author(s) and the title of the work, journal citation and DOI.
Published under licence by IOP Publishing Ltd

the photoresponse of TiO_2 to visible region, including elements dopping (transition metals or non-metals) and nanoparticle surface modification (noble metals and transition metal oxides).[13-16] Reseach proves that surface modification is more suitable to overcome the issues than element dopping (suffering from thermal instability, photo-corrosion, lattice distortion, and an increase in the carrier-recombination probability).[17] Coupling TiO_2 with other narrow bandgap semiconductors serving as the sensitizer is considered as an efficient way to absorb visible light.[9, 18]

Core-shell structures, as one of the most important way for surface modification, have obtained intensive research interests due to representing diverse functions related components integrated into one unit and widely applying in renewable energy, advanced biomedicine, and environmental protection.[19-21] The successful applications of core-shell structures depend upon the availability of various shell frameworks with tunable composition, thickness, and structure over well-designed functional cores.[22] The core-shell structures, especially TiO_2 as shell, are also well applied in photocatalysis owning to their fascinating features. The cores play important roles in trapping photogenerated electrons and tuning the bandgap of the TiO_2 shell.[23-25]

In_2O_3, a semiconductor with a direct bandgap of 3.6 eV and an indirect bandgap of 2.8 eV, is proposed as an efficient sensitizer to extend the absorption spectra of oxide semiconductors from UV region to the visible region.[26, 27] As aforementioned, In_2O_3 as the core, coupling with TiO_2 can transfer electrons from an excited small bandgap semiconductor to another one in the case of proper conduction band potentials, which benefits the separation of photogenerated electrons and holes and further enhancing the photocatalytic activity. This can be attributed to the difference of bandgaps between In_2O_3 (~2.8 eV) and TiO_2 (~3.2 eV for anatase). More importantly, an efficient heterostructure for separation of photoinduced charge carries can be formed via the higher conduction band (CB) of In_2O_3 (E_{CB} = -0.63 V vs. NHE) than that of TiO_2 (E_{CB} = -0.4 V vs. NHE).[28, 29]

Based on this feature, different morphologies of In_2O_3-TiO_2 photocatalysts have been synthesized, including surface-modified nanoparticles, films, and so on.[30, 31] Among these materials, In_2O_3-TiO_2 core-shell structure is proposed as a promising structure for the purpose of speeding up electron transfer and preventing recombination of electron-hole pairs.[28] However, it is little reported on the core-shell structures with fast electron transfer, low recombination rate, and high surface area.

Herein, we demonstrate a simple method to fabricate porous In_2O_3-TiO_2 core-shell spherical nanocomposites by controlling the ratio of titanium precursors to In_2O_3 nanospheres in acetone solution. No high-temperature calcination for crystallization of porous TiO_2 is one of the highlights for this coating method. The products are characterized by several advanced techniques, such as XRD, TEM, SEM, and UV-vis spectroscopy. Finally, the photocatalytic activity of the as-prepared core-shell structures is evaluated by degradation of methyl blue under simulated solar light irradiation.

2. Experimental

2.1. Preparation of In_2O_3 nanospheres

The In_2O_3 nanospheres were prepared by hydrothermal methods and followed by calcination in air. In a typical procedure, 10 ml 0.2 M NH_4HCO_3 solution was generally mixed with the equivalent volume of 0.05 M $InCl_3$•$4H_2O$ solution. 0.2 g Na_2SO_4 and 1 mmol citrate acid were added into the previous mixture solution. After vigorous stirring, the mixed precursor solution was transferred into a 20 ml Teflon-lined stainless autoclave, sealed and maintained at 160 ℃ for 8 h, then cooled down to room temperature. The as-prepared products were collected by centrifuge and washed several times with ethanol and deionized water, respectively. Finally, the products were dried at 70 ℃ for 12 h.

2.2. Preparation of In_2O_3@TiO_2 core-shell spherical nanocomposites

30 mg of In_2O_3 nanospheres was added in 150 ml acetone to form a suspension. Afterward, a certain amount of 0.5 vol.% titanium butoxide (TBT) ethylene glycol solution was added into the previous suspension. After sonication for a while and followed with standing for 8 h, the as-prepared participates were collected and washed for further use. For crystallization, the precursors were boiled

in ultrapure water for 2 h. And then, the products were centrifuged and washed with DI water and ethanol for several times and dried at 70 ℃ for several hours.

2.3. Characterization

The compositions of the as-prepared products were characterized by Phillips X'pert Multipurpose X-ray Diffraction System (MPD) in the 2θ range of 5-80 °. SEM images were recorded with a Zeiss field emission scanning electron microscope. The composite morphologies were observed on an FEI tecnai G20 microscope (TEM), operated at an accelerated voltage of 100 kV. The Brunauer-Emmett-Teller (BET) surface area and pore size with the distribution of the products were obtained from nitrogen physisorption isotherms (adsorption-desorption branches) at 77 K on a Micromeritics ASAP 2020 instrument. The optical properties were obtained on a Shimadzu UV-2600 UV-vis spectrophotometer (Varian) with a 1 cm quartz cell.

2.4. Photocatalysis test

The photocatalytic activities of TiO_2 based core-shell nanocomposites were determined by measuring the decolorization of MO under simulated solar light irradiation in a batch reaction. The reactor volume is 250 ml. A 300W xenon lamp (PLS-SXE300C) equipped with AM 1.5G total reflection filters was used to obtain simulated solar light to trigger the photocatalytic reaction, and the lamp was positioned about 15 cm away from the reactant solution meniscus. The luminance of the light source over the reactant solution was 0.7 W/cm^2. A 100 ml solution of 30 ppm methylene blue (MB) was injected into the reaction system, while 0.020 g of the photocatalyst was added. Prior to irradiation, the suspension was magnetically stirred in the dark for 30 min to ensure adsorption-desorption equilibrium. At given time intervals, 3 ml solution was sampled and filtrated to remove the catalysts. The filtrates were analyzed by recording the variations of the absorption band maximum (657 nm) of methyl orange using a Shimadzu UV-2600 UV-Vis spectrophotometer. After various time intervals, MB concentration could be estimated using the following equation:

$$\text{MB concentration} = C/C_0 \times 100\% \quad (1)$$

Where C_0 is the initial MB absorbance at 664 nm and C is the absorbance obtained after various intervals of time. The reaction rate (k) could be estimated as the linear relationship between $\ln(C/C_0)$ and time:

$$\ln(C/C_0) = kt \quad (2)$$

To eliminate the effect of heating during irradiation, the reactor was equipped with reflux condensation. After decolorization, the supernatant of the solution was obtained via centrifugation, and then characterized by UV-Vis spectroscopy.

3. Results and discussion

3.1. Morphology and composition

The composition of the In_2O_3@TiO_2 core-shell nanocomposites and pure In_2O_3 nanospheres were characterized by XRD techniques. Fig. 1 shows the XRD patterns of the pure In_2O_3 nanospheres (green line) and the nanocomposites obtained at various molar ratios of In_2O_3 to TiO_2. For pure In_2O_3 nanoparticles, the XRD pattern indicates the diffraction peaks of cubic In_2O_3 (JCPDS NO. 01-089-4595), which is in good agreement with the previous study.[28, 29] In the patterns of nanocomposites, the peaks corresponding to TiO_2 appear, and the diffraction peaks centered at 2θ = 25.3 °, 48.6 °, and 53.8 °is consistent with the peaks of (101), (200), and (105) from anatase TiO_2.[28, 30] In addition, the intensity of the TiO_2 (101) peaks apparently increase with the ratios. No other peaks related to impurities are observed, which indicates the high purity of the products.

The morphologies of the pure In_2O_3 nanospheres and In_2O_3@TiO_2 core-shell nanocomposite are recorded by SEM and TEM, respectively. Fig. 2 a & b shows the SEM and TEM image of the pure

In_2O_3 nanospheres. It can be seen that the nanospheres with the diameters of ~200 nm are uniform and with smooth surfaces. Fig.2 c-f shows the In_2O_3@TiO_2 core-shell nanospheres prepared at different molar ratios of In to Ti (from 1:5 to 1:15). The spherical particles with high contrast represent In_2O_3 as cores, and the low contrast part corresponds to porous TiO_2 polycrystalline as the shell. It can be seen that TiO_2 are well coated on the In_2O_3 nanospheres, and the thickness of the shell increases with the molar ratios of In to Ti (20, 40, 50, and 70 nm for the ratios of 1:5, 1:7, 1:10, and 1:15). The thickness of the shell may affect the future functional performance.

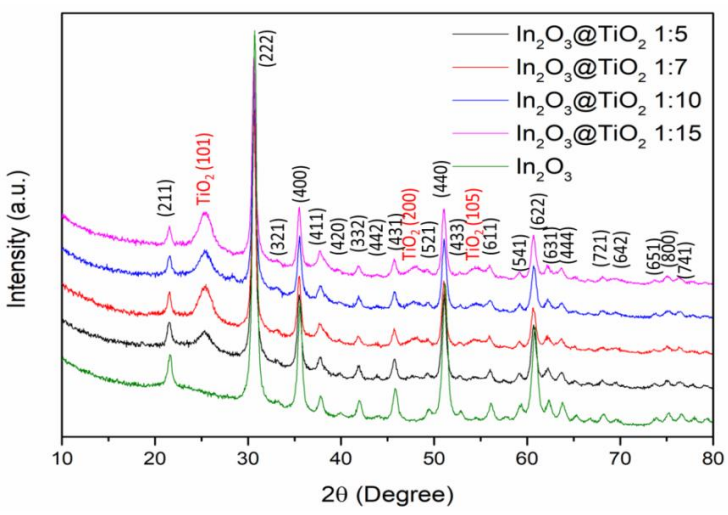


Figure 1. XRD patterns of pure In_2O_3 and In_2O_3@TiO_2 core-shell nanostructures with various molar ratios (from 1:5 to 1:15).

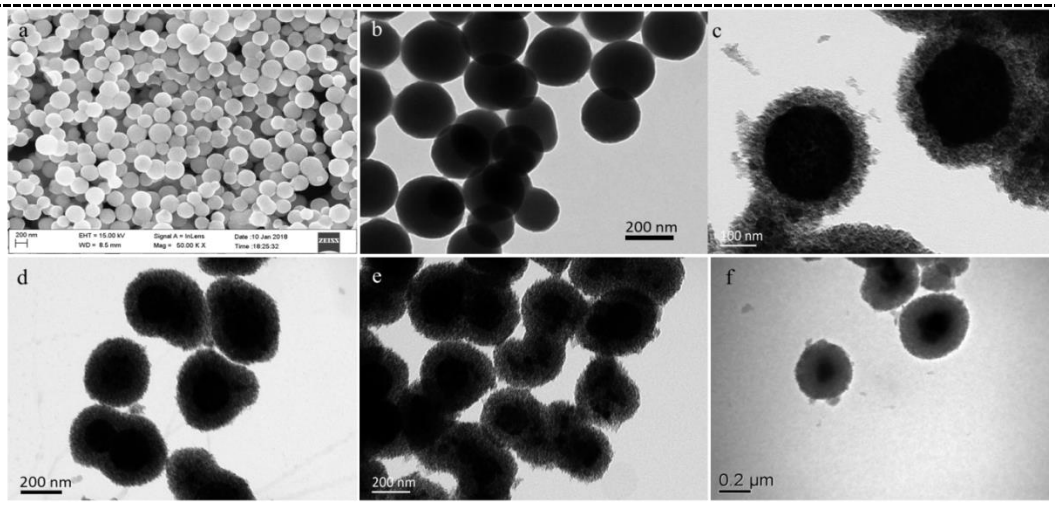


Figure 2. (a, b) SEM and TEM image of the pure In_2O_3 nanospheres; TEM images of In_2O_3@TiO_2 core-shell nanostructures obtained with various molar ratios of (c) 1:5, (d) 1:7, (e) 1:10, and (f) 1:15.

3.2. Optical properties

The optical properties of the nanoparticles prepared in this study, including pure In_2O_3 nanospheres and the In_2O_3@TiO_2 core-shell nanocomposites synthesized at various molar ratios of In to Ti, were measured and analyzed. The UV-Vis spectra of the nanoparticles are shown in Fig. 3. It can be seen

that there is no obvious surface plasmon resonance for pure In_2O_3 and TiO_2 particles in the rage of 200 to 800 nm. The peak of TiO_2 is located at 319 nm while the In_2O_3 are centered at 323 nm. This is in accordance with the literature.[32] After coating with TiO_2, the peaks of the nanocomposites are slightly shifted to long wavelength by ~20 nm. The adsorption peaks become broaden probably due to the larger size after coating.[18] In addition, the locations of the peaks are little changed with the ratios. Specifically, the peaks are centered at 342, 399 and 337 nm for the ratio of 1:10, 1:15, and 1:5, respectively.

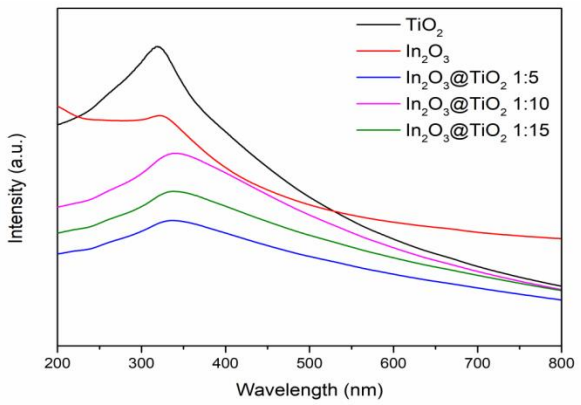


Figure 3. UV-Vis spectra of the pure TiO_2, pure In_2O_3 nanospheres, and the core-shell nanocomposites.

3.3. Photocatalytic activity

The photocatalytic activities of the pure In_2O_3 nanospheres and the core-shell nanocomposites were measured by the degradation of 30 ppm MB solution. Fig. 4 shows the corresponding concentration changes of the MB solution and the reaction rate constant as a function of simulated solar light exposure time. In the case of pure In_2O_3 and TiO_2 as photocatalysts, ~70% and 74% degradation of MB can be obtained in 250 min after exposure to the solar light. In comparison, the as-preparation In_2O_3@TiO_2 core-shell nanocomposites show that the degradation of > 95% MB can be achieved under similar conditions. It should be noted that the photocatalytic activities under solar light irradiation of all the hybrid nanocomposites are superior to those of pure In_2O_3 and TiO_2. However, the photocatalytic performances of the nanocomposites are similar. Specifically, nearly 100% degradation of MB can be obtained at the molar ratio of 1:10, which shows the best photocatalytic activity towards the degradation of MB under solar light illumination, followed with the In_2O_3@TiO_2 core-shell nanocomposites with the ratios of 1:5 and 1:15. It can be noticed that smaller amount of TiO_2 coating improves the photocatalytic activity of the whole In_2O_3@TiO_2 core-shell nanocomposites. Fig.4b shows the reaction rate constants of all tested samples, and the core-shell nanocomposites at the ratios of 1:10 shows the highest rate constant among all the samples. The photocatalytic activity and the kinetic rate constants of all the different photocatalysts follow the order: 1:10 core-shell structure ($k = 0.0152\ min^{-1}$) > 1:5 ($k = 0.0146\ min^{-1}$) > 1:15 ($k = 0.0127\ min^{-1}$) > pure In_2O_3 ($k = 0.0069\ min^{-1}$) > pure TiO_2 ($k = 0.0058\ min^{-1}$). This may be related to the surface area and the thickness of various amounts of TiO_2 coating. The surface areas measured by BJH method via adsorption isotherm are 168, 177, 171 m^2/g, which are close to that of pure TiO_2 (180 m^2/g)[33] but much higher than that of pure In_2O_3 nanospheres (120 m^2/g). The similar surface area of the nanocomposites and pure TiO_2 is because the contribution of the surface area is mainly from TiO_2. Normally, the large surface area can provide more adsorption site of dye molecules, and further increase the photocatalytic activity. The increase of the shell thickness is little affected the photocatalytic performance, which supports the relationship between performance and surface areas.

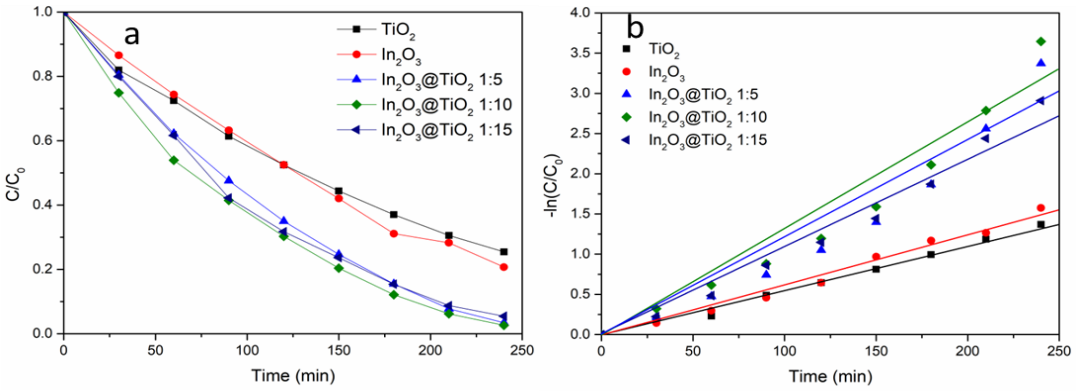


Figure 4. (a) Degradation rates of MB in the presence of the photocatalysts under simulated solar light irradiation. (b) Apparent rate constants of different photocatalysts.

3.4. Mechanism

The factors affecting the photocatalytic activity are diverse, such as surface area, bandgap energy, particle size, and the electron-hole recombination rate. The catalytic properties under solar light irradiation are mainly dependent upon the bandgap structure for the core-shell nanocomposites.[34] When In_2O_3 nanospheres are coupled with TiO_2 particles, the Fermi level of TiO_2 and In_2O_3 must align in equilibrium due to the existence of the In_2O_3/TiO_2 heterojunction.[35, 36] Under solar light irradiation, the photo-generated electrons transfer from the conduction band of In_2O_3 to the conduction band of TiO_2 under the built-in electric field, and the concentration gradient activated and yielded charge carriers, while the photo-generated holes accumulated in the valence band of In_2O_3. The negative electrons in the valence band of TiO_2 reacted with O_2 molecules in the aqueous solution and form the superoxide ions (O_2^-) and hydrogen peroxide (H_2O_2), while the holes react with OH^- and produce reactive hydroxyl radicals (•OH).[29, 31]

4. Conclusions

In this study, the $In_2O_3@TiO_2$ core-shell spherical nanocomposites have been synthesized via a hydrothermal method for preparation of In_2O_3 nanospheres and sol-gel method for coating TiO_2 shell. The coating method shows several unique advantages, such as rapid and effective surface coating for materials and morphologies, no need of high temperature (>100 ℃), and potential for scale-up production. The core-shell nanocomposites have been proved as excellent solar-light-driven photocatalysts showing superior photocatalytic activity to the pure TiO_2 and In_2O_3 nanospheres. The red-shift of the nanocomposites, compared with pure TiO_2 nanoparticles, is attributed to the combination of the narrow bandgap of In_2O_3. The existence of the In_2O_3/TiO_2 heterojunction and the matched energy hands of this core-shell structure benefit the charge transfer and suppress rapid recombination of photo-generated electrons and holes. This study offers potentially advanced core-shell nanocomposites in photocatalysis for practical use.

Acknowledgement

We gratefully acknowledge the financial support National Natural Science Foundation of China (No. 51704070) and the Fundamental Research Funds for the Central Universities of China (N172504028).

References

[1] Rahimi N, Pax R A and Gray E M 2016 *Prog Solid State Ch* **44** 86-105
[2] Ray C and Pal T 2017 *Journal of Materials Chemistry A* **5** 9465-9487
[3] Fujishima A and Honda K 1972 *Nature* **238** 37
[4] Ao C H and Lee S C 2005 *Chem Eng Sci* **60** 103-109

[5] Zhong L, Lee C S and Haghighat F 2012 *J Hazard Mater* **243** 340-349
[6] Schneider J, Matsuoka M, Takeuchi M, Zhang J, Horiuchi Y, Anpo M and Bahnemann D W 2014 *Chemical Reviews* **114** 9919-9986
[7] Nakata K and Fujishima A 2012 *Journal of Photochemistry and Photobiology C: Photochemistry Reviews* **13** 169-189
[8] Gueymard C A 2004 *Sol Energy* **76** 423-453
[9] Yang X H, Fu H T, An X Z, Jiang X C and Yu A B 2016 *RSC Advances* **6** 34103-34109
[10] Moniz S J A, Shevlin S A, An X, Guo Z-X and Tang J 2014 *Chemistry – A European Journal* **20** 15571-15579
[11] Shao X, Lu W, Zhang R and Pan F 2013 *Scientific Reports* **3** 3018
[12] Xu Y-J, Zhuang Y and Fu X 2010 *The Journal of Physical Chemistry C* **114** 2669-2676
[13] Wang F, Ban P-P, Parry J P, Xu X-H and Zeng H 2016 *Rare Metals* **35** 940-947
[14] Jianyu Y, Lin Z, Yang W, Yingling T, Zhenlin W, Shining Z and Jia Z 2018 *Journal of Optics* **20** 034005
[15] Filippo E, Carlucci C, Capodilupo A L, Perulli P, Conciauro F, Corrente G A, Gigli G and Ciccarella G 2015 *Materials Research* **18** 473-481
[16] Dong P, Liu B, Wang Y, Pei H and Yin S 2011 *J Mater Res* **25** 2392-2400
[17] Asahi R, Morikawa T, Ohwaki T, Aoki K and Taga Y 2001 *Science* **293** 269-271
[18] Fu H, Sun S, Yang X, Li W, An X, Zhang H, Dong Y, Jiang X and Yu A 2018 *Powder Technology* **328** 389-396
[19] Joo S H, Park J Y, Tsung C-K, Yamada Y, Yang P and Somorjai G A 2008 *Nature Materials* **8** 126
[20] Xiong Z and Zhao X S 2012 *J Am Chem Soc* **134** 5754-5757
[21] Ghosh Chaudhuri R and Paria S 2012 *Chemical Reviews* **112** 2373-2433
[22] Li W, Yang J, Wu Z, Wang J, Li B, Feng S, Deng Y, Zhang F and Zhao D 2012 *J Am Chem Soc* **134** 11864-11867
[23] Khashan S, Dagher S, Tit N, Alazzam A and Obaidat I 2017 *Surface and Coatings Technology* **322** 92-98
[24] Vaidya S, Patra A and Ganguli A K 2010 *Colloids and Surfaces A: Physicochemical and Engineering Aspects* **363** 130-134
[25] Lee J-W, Kong S, Kim W-S and Kim J 2007 *Mater Chem Phys* **106** 39-44
[26] Di Quarto F, Sunseri C, Piazza S and Romano M C 1997 *The Journal of Physical Chemistry B* **101** 2519-2525
[27] Shchukin D, Poznyak S, Kulak A and Pichat P 2004 *Journal of Photochemistry and Photobiology A: Chemistry* **162** 423-430
[28] Mu J, Chen B, Zhang M, Guo Z, Zhang P, Zhang Z, Sun Y, Shao C and Liu Y 2012 *ACS Applied Materials & Interfaces* **4** 424-430
[29] Zhou X, Wu J, Li Q, Zeng T, Ji Z, He P, Pan W, Qi X, Wang C and Liang P 2017 *J Catal* **355** 26-39
[30] Petronella F, Rtimi S, Comparelli R, Sanjines R, Pulgarin C, Curri M L and Kiwi J 2014 *Journal of Photochemistry and Photobiology A: Chemistry* **279** 1-7
[31] Garcia L M P, Tavares M T S, Andrade Neto N F, Nascimento R M, Paskocimas C A, Longo E, Bomio M R D and Motta F V 2018 *Journal of Materials Science: Materials in Electronics* **29** 6530-6542
[32] Li Z, Zhang P, Shao T, Wang J, Jin L and Li X 2013 *Journal of Hazardous Materials* **260** 40-46.
[33] Yang X, Fu H, Yu A and Jiang X 2012 *J Colloid Interf Sci* **387** 74-83
[34] Du J, Lai X, Yang N, Zhai J, Kisailus D, Su F, Wang D and Jiang L 2011 *Acs Nano* **5** 590-596.
[35] Lin C J, Liou Y H, Zhang Y, Chen C L, Dong C-L, Chen S-Y and Stucky G D 2012 *Applied Catalysis B: Environmental* **127** 175-181
[36] Yang X, Cao C, Erickson L, Hohn K, Maghirang R and Klabunde K 2009 *Applied Catalysis B: Environmental* 91 657-662